Activation of the hippocampal CA1 astrocyte Gq and Gi G protein-coupled receptors exerts a protective effect against attention deficit hyperactivity disorder

Yu-Dong Shan

Hebei Province Cangzhou Hospital of Integrated Traditional and Western Medicine

Zhi-Fang Yu

Hebei Province Cangzhou Hospital of Integrated Traditional and Western Medicine

Ge-Ge Lv

The First Affiliated Hospital of Zhengzhou University

Yong-Lin Shan

Hebei Province Cangzhou Hospital of Integrated Traditional and Western Medicine

Bao-Dong Li

Hebei Province Cangzhou Hospital of Integrated Traditional and Western Medicine

Jian-Yong Zhao

Hebei Province Cangzhou Hospital of Integrated Traditional and Western Medicine

Xiao-Ming Li

Hebei Province Cangzhou Hospital of Integrated Traditional and Western Medicine

Wei-Juan Gao

Hebei University of Chinese Medicine

Li-Min Zhang

azai2010@126.com

Hebei Province Cangzhou Hospital of Integrated Traditional and Western Medicine

---

Research Article

Additional Declarations: No competing interests reported.

Abstract

Background

Attention deficit hyperactivity disorder (ADHD) is characterized by symptoms such as inattention, hyperactivity and impulsiveness, which significantly impact the healthy development of children. Our prior research demonstrated that exposure to S-Ketamine during pregnancy can lead to the development of ADHD, and existing studies have established a close association between astrocytes and the onset and progression of ADHD. The activation and inhibition of astrocytes are closely linked to neuropsychiatric dysfunction, and astrocytic NOD-like receptor protein 3 (NLRP3) has been reported to contribute to alterations in mental state and cognitive deficits. Thus, this study aims to investigate the role of astrocytes in ADHD by selectively modulating astrocyte function through Gq and Gi G protein-coupled receptors (GPCRs) and by specifically targeting the knockout of NLRP3.

Methods

Pregnant C57BL/6J mice or mice with a specific deletion of NLRP3 in astrocytes were administered intraperitoneal injections of 15 mg/kg of S-ketamine for 5 consecutive days from gestational day 14 to 18 to establish an ADHD model. To modulate astrocyte activity in the hippocampal CA1 region, we administered astrocyte-specific Gq-Adeno-associated virus (AAV) or Gi-AAV into the CA1 and maintained treatment with CNO. At 21 days postnatally, we conducted open field test (OFT), novel object recognition (NOR), elevated plus maze (EPM) and fear conditioning (FC) in the offspring mice. Additionally, on postnatal day 14, we implanted electrodes in the CA1 region of the offspring mice for neurophysiological monitoring and investigated local field potentials (LFP) during novel object exploration on postnatal day 21. Lastly, pathological assessments were conducted after euthanasia.

Results

Both the activation and inhibition of astrocytes in the hippocampal CA1 region improved impulsive-like behaviors and cognitive function in ADHD mice, reduced the power of theta (θ) oscillations during novel object exploration and decreased NLRP3-associated inflammatory factors, including cleaved caspase-1 and IL-8. Furthermore, compared to WT mice, astrocyte-specific NLRP3 conditional knockout mice demonstrated significantly reduced impulsive behavior and cognitive deficits, as well as a decrease in θ oscillation power and a reduction in NLRP3-associated inflammatory factors.

Conclusions

Our data provide compelling evidence that the activation of astrocytic Gq or Gi pathways improves ADHD-like behaviors through NLRP3-dependent mechanisms.

1. Introduction

Attention Deficit Hyperactivity Disorder (ADHD) is characterized by symptoms including inattention, hyperactivity and impulsivity[1], which affects approximately 5% of children and adolescents worldwide[2]. ADHD not only has significant implications for academic performance and social relationships during childhood but may also persist into adulthood. Untreated individuals with ADHD may face a range of negative consequences, including academic underachievement, occupational instability, substance abuse, and mental health issues[3, 4]. Consequently, investigating the pathogenesis of ADHD and developing effective strategies for its prevention and treatment have become crucial research endeavors in the medical field.

In our previous work, we established an ADHD model by administering prenatal S-ketamine injections[5], and the results revealed that compared to neurons and microglia, astrocytes, particularly in the CA1 region of the hippocampus, exhibited significant activation[5]. Astrocytes are an important cell type in the central nervous system, and their role has received significant attention in neurological disease research[6]. Activation of astrocytes through Gq G protein-coupled receptors (GPCRs) modulates astrocyte activity and influences the pathophysiology of neurological disorders[7]. Previous studies have demonstrated that chronic activation of Gq GPCRs in astrocytes can induce changes in locomotor and anxiety-related behaviors[8]. Additionally, acute activation of Gq GPCRs in astrocytes has a significant impact on the autonomic nervous system and behavior[9], and research has shown that Gi GPCR activation in astrocytes can prevent Stress-enhanced Fear Learning from developing[10]. It has not yet been documented, yet, how astrocyte Gq and Gi GPCR activation contributes to the development and course of ADHD. We concentrated on the CA1 area of the hippocampus because it has been frequently linked to contextual memory[11] and because neurons in this region have shown learning-dependent potentiation[12]. Additionally, working memory deficits are among the symptoms associated with ADHD in children[13]. A notable decrease in long-term potentiation at the CA1 hippocampal synapse linked to working memory impairment has been found using a mouse model of ADHD brought on by prenatal nicotine exposure[14]. Furthermore, studies have shown that the regulation of astrocytes in the CA1 region can enhance memory and cognitive abilities[15]. Thus, in this study, we focused on the CA1 region for these compelling reasons.

A major risk factor for ADHD is neuroinflammation[16]. Maturation of caspase-1 is brought about by the activation of NLRP3 inflammasomes, and caspase-1 mediates the conversion of pro-IL-18 into mature and active IL-18. Notably, studies have suggested that inhibiting the NLRP3 pathway could serve as a therapeutic approach for ADHD[17, 18]. In a recent report, we established a link between the inhibition of the NLRP3-IL-18 signaling pathway in astrocytes and emotional alterations following traumatic stress[19]. Intriguingly, prior studies have demonstrated that both the activation of Gq and Gi GPCRs can manifest anti-inflammatory effects[20, 21]. However, it remains unclear whether the activation of astrocytes via the NLRP3 signaling pathway is involved in the progression of ADHD.

In this study, we introduced adeno-associated viruses into the CA1 region of the hippocampus in ADHD mice to stimulate astrocytic Gq and Gi GPCRs. Our findings strongly indicate that activating astrocytic Gq and Gi GPCRs may alleviate hyperactive impulsive-like behavior in ADHD mice, possibly by inhibiting the NLPR3-induced inflammatory response through the activation of Gq and Gi GPCRs.

2. Materials and methods

The Hebei Province Cangzhou Hospital of Integrated Traditional and Western Medicine's Institutional Animal Care and Use Committee authorized all experimental techniques used in this study (No. CZX2023-KY-023). The Animal Research: Reporting of In Vivo Experiments (ARRIVE) principles were also followed by the study methodology.

2.1 Animals and models

Specific pathogen-free (SPF) grade C57BL/6 mice (Liaoning Changsheng Biotechnology Co., LTD(SCXK(L)2020-0001) weighing 25–28 g were used. To generate SPF grade NLRP3 conditional knockout (NLRP3-cKO) mice of similar weight, we bred NLRP3$^{f/f}$ mice with GFAP-Cre transgenic mice (Saiye Biotechnology Co., Ltd., SCXK(S)2020-0006). NLRP3$^{f/f}$ mice were obtained from mating NLRP3$^{f/w}$ mice. Genomic DNA from tail biopsies was genotyped using specific PCR primer sets. The NLRP3 floxed allele was detected using F2 (5'-TTGTGGAGGATGGGAAGTCTAAAG-3') and R2 (5'-CTCAGATAGACACCATCGTCTCAG-3'), yielding a 191-bp band for the wild-type allele and a 251-bp band for the NLRP3 floxed allele. The presence of the Cre gene was confirmed with F5 (5'-GAACGCACTGATTTCGACCA-3') and R5 (5'-GCTAACCAGCGTTTTCGTTC-3'), resulting in a 204-bp Cre amplicon.

During the experiment, the mice were individually housed in cages containing wood chips, maintaining a controlled environment with a temperature range of 23–25°C, a 12-hour light-dark cycle, and humidity levels ranging from 40–60%. They were provided with ad libitum access to both food and water. Following the methodology outlined in our previous work[5], we implemented the following procedures for modeling: Male and female mice were co-housed, and the day when vaginal plugs and sperm were detected was designated as gestational day 0.5 (G0.5). Gestational age was calculated using crown-rump length (CRL) measurements obtained with a 40 MHz high-resolution linear sensor using the formula (CRL/2 + 9). From G14 to G18, pregnant mice were intraperitoneally injected with S-Ketamine (15 mg/kg, Hengrui Pharmaceutical Co., Ltd.) for five consecutive days. After 21 days following birth, all offspring mice were weaned.

2.2 Group assignment

From gestational day 14 (G14) to G18, the offspring mice were given intraperitoneal injections of S-Ketamine for five consecutive days to establish an ADHD model. In the initial stage, the offspring ADHD mice were randomly divided into three groups: (1) ADHD (n = 48), (2) ADHD + rAAV-GfaABC1D-hM3D(Gq)-mCherry + CNO (ADHD + hM3Dq) (n = 48), and (3) ADHD + rAAV-GfaABC1D-hM4D(Gi)-mCherry + CNO

(ADHD + hM4Di) (n = 48). In the second stage, the offspring ADHD mice were randomly assigned to two groups: (1) WT + ADHD (n = 48) and (2) NLRP3-cKO + ADHD (n = 48).

2.3 Stereotactic injection of virus

On postnatal day 14, the mice were anesthetized in an induction chamber pre-filled with 5% sevoflurane (21082531, Shanghai Hengrui Pharmaceutical Co., Ltd., Shanghai, China). After the loss of reflexes, they were removed from the chamber and placed in a single-number stereotaxic instrument (Beijing Zhongshi Di Chuang Development Technology Co., Ltd., Beijing, China) while lying in the prone position. To prevent eye dryness, vitamin A palmitate ophthalmic gel (220101, Shenyang Xingqi Pharmaceutical CO., LTD., Shenyang, China) was applied to both eyes of the mice. Subsequently, the hair was removed, and the area was disinfected. Local anesthesia was achieved by infiltrating the scalp with 0.5% lidocaine (1B210716107, Hebei Tiancheng Pharmaceutical Co., Ltd., Hebei, China). A longitudinal incision was made in the scalp to expose the skull, followed by the removal of the periosteum to reveal the skull surface. Small holes were then drilled at coordinates 1.38 mm posterior to the bregma and 1.3 mm lateral to the midline on each side. Glass electrodes were inserted through these small holes to a depth of 1.6 mm from the cortical surface, reaching the hippocampal CA1 region. Subsequently, rAAV-GfaABC1D-hM3D(Gq)-mCherry (Titer: 3.05E + 12 VG/ml, BC-0908, Brain Case, Shenzhen, China) or rAAV-GfaABC1D-hM4D(Gi)-mCherry (Titer: 3.00E + 12 VG/ml, BC-0907, Brain Case, Shenzhen, China) was injected at a controlled rate of 50 nl/min, totaling 200 nl. After the injection, the needle was kept in place for 10 minutes before being slowly withdrawn from the glass electrode. Lastly, the incision in the skull was sealed using bone wax, and the skin incision was sutured.

2.4 Preparation of clozapine N-oxide

To prepare a stock solution of clozapine N-oxide (CNO) (S6887, Selleck Chemicals, USA), 50 mg of CNO was dissolved in 10 ml of dimethyl sulfoxide (DMSO) (ST038, Beyotime, Shanghai, China), resulting in a CNO stock solution with a concentration of 5 mg/ml. This CNO stock solution was subsequently diluted to create a working solution with a concentration of 0.25 mg/ml using physiological saline for intraperitoneal administration. Thirty minutes before conducting behavioral tests, intraperitoneal injections of CNO were administered at a dose of 2.5 mg/kg.

2.5 Open feld test (OFT)

On postnatal day 21, OFT was conducted. Briefly, the mice were placed in the right-bottom corner of a transparent square acrylic container measuring 60 cm × 60 cm × 60 cm, and their activity and their total distance traveled were recorded using a camera for 5 minutes. The Super Maze Tracking System (XR-XZ301, Shanghai Xinruan Software Co., Ltd., Shanghai, China) was used to analyze the average speed and time spent in the center zone. After the test, the apparatus was cleaned with 75% alcohol to eliminate any potential odor interference in subsequent experiments.

2.6 Elevated plus maze (EPM)

On postnatal day 21, the EPM test was conducted. Briefly, the mice were gently placed head-first into the center of an elevated plus maze with four arms (2 open arms and 2 closed arms, each measuring 30 cm × 8 cm × 15 cm). Their movements were recorded using a camera for 5 minutes. Subsequently, the Labmaze tracking system (Labmaze V3.0, Beijing Zhongshi Di Chuang Development Technology Co., Ltd., Beijing, China) was used to analyze the number of entries and the time spent in the open arms.

2.7 Novel object recognition (NOR)

On postnatal days 21 and 22, we performed the NOR test. On the first day, the mice were allowed to explore two identical cubic objects in the left and right corners of a black box (measuring 60 cm × 60 cm × 40 cm) for 5 minutes. On the second day, the cubic object on the right was replaced with a novel spherical object. During this phase, continuous monitoring for 5 minutes was conducted using the Supermaze tracking system.

2.8 Fear conditioning (FC)

On postnatal days 21 and 22, the FC test was conducted. On the first day, the mice were placed in a conditioned fear test chamber (Beijing Zhongshi Di Chuang Development Technology Co., Ltd., Beijing, China) and exposed to three tone-foot shock pairings consisting of a tone (2000 Hz, 80 dB, 60 s) followed by a foot shock (1 mA, 2 s). After the final foot shock, the offspring mice were kept in the chamber for an additional 60 seconds. On the following day, the offspring mice were placed in the same chamber but without any tone-foot shock pairings for 3 minutes. Two hours later, they were transferred to a new chamber with different environmental conditions (transparent walls and lighting), and an added odor (applied by wiping with 1% acetic acid), and their "freezing" behavior was then recorded.

2.9 In vivo Neurophysiological Monitoring

On postnatal days 21 and 22, we implanted a 16-channel microelectrode array (Kedouc, Suzhou, China) in the mice (n = 6) using the following procedures: The mice were placed in an anesthesia chamber pre-filled with 3% sevoflurane, and once they exhibited no reflex responses, they were securely positioned in a stereotaxic apparatus, and anesthesia was maintained with 3% sevoflurane. Following skin disinfection using 75% alcohol, the fur on the mice's heads was removed, and a skin incision was made. Gentle dissection was conducted to expose the dura mater and the skull. Using a small animal high-speed cranial drill, we created a circular hole with a diameter of 1.5 mm at coordinates AP = -1.38 mm, ML = + 1.3 mm. Then, we carefully removed the dura mater, and the microelectrode array was slowly inserted into the hippocampal CA1 region of the brain (DV = 1.6 mm) using forceps. Dental cement was used to secure the electrodes in place. After the surgery, the mice were carefully relocated and kept in a warm environment for recovery, and once their vital signs stabilized, they were returned to their original cages. Seven days after the recovery period, we conducted the NOR experiment and recorded field potentials 1 second before and after the mice first entered the new object area using NeuroStudio (Jiangsu Brain Medical Technology Co. Ltd, China). Brainwave data were subsequently subjected to LFP analysis using Neuroexplorer (Plexon Instruments, USA).

To further evaluate the functional status of the hippocampus, we conducted in vivo neurophysiological monitoring to assess activity in the CA1 region of the hippocampus when mice encountered a novel object. Specifically, during the second phase of CNO administration, we recorded alterations in θ oscillation power (4–7 Hz) in the hippocampal CA1 region 1 second before and after the mice entered the novel object area.

2.10 Immunofluorescence

Under sevoflurane anesthesia, the mice were perfused with ice-cold physiological saline and 10% neutral buffered formalin through the left ventricular aorta, after which they were decapitated, and their brain tissues were extracted. A mouse brain slicer was then used to create vertical slices located approximately 2 mm posterior to the mouse brain's bregma, with a thickness of approximately 1 mm. Subsequently, these slices underwent a process of dehydration and embedding. The tissue sections were taken and sliced into 4 µm-thick sections, which were subsequently embedded in paraffin wax. Antigen repair was conducted after treating the sections with sodium citrate, followed by blocking with Quickblock (P0260, Beyotime, Shanghai, China). The slices were incubated overnight at 4°C with monoclonal antibodies against GFAP (1:100, GB11096-100, Servicebio, Wuhan, China), GAD65 (1:100, ab239372, Abcam, Cambridge, UK), PSD95 (1:100, WL05046, Wanleibio, Shenyang, China), IL-18 (1:100, AF7266; Beyotime, Shanghai, China), and cleaved-caspase1 (1:100, AF4022; Affinity, San Diego, USA). On the subsequent day, the slices were exposed to secondary antibodies (CyTM3-conjugated goat anti-mouse IgG, 1.5 mg/mL, A0521, Beyotime; and FITC-conjugated goat anti-rabbit IgG, 1.5 mg/mL, A0562, Beyotime) in the dark for 1 hour. Nuclei were stained with 5 µg/mL of DAPI (P0131; Beyotime) following rinsing with PBS. A pathologist, blinded to the grouping, assessed the above slices using a confocal laser microscope (CSIM110, Sunny, Beijing, China). An average of six fields with a magnification of 200x were randomly selected on six slices, and the intensity of GFAP, GAD65 and PSD95, as well as the areas occupied by cleaved caspase-1 and IL-18 in GFAP positive cells, were analyzed using Image-Pro Plus 6.0 (NIH, Bethesda, MD, USA).

Under sevoflurane anesthesia, the mice were subjected to perfusion with ice-cold physiological saline and 10% neutral buffered formalin through the left ventricular aorta. Subsequently, the brains were carefully extracted, postfixed overnight in 4% PFA at 4°C, and cryoprotected by incubating them in 30% sucrose in PBS. The brains were then sectioned to a thickness of 30 µm using a sliding freezing microtome (SM2000R, Leica, Wetzlar, Germany). After this, antigen repair was conducted following treatment with sodium citrate, and the sections were blocked with Quickblock (P0260, Beyotime, Shanghai, China). The nuclei were stained with 5 µg/mL of DAPI (P0131; Beyotime, Shanghai, China) after rinsing with PBS. Then, a pathologist blinded to the grouping assessed the above slices using a confocal laser microscope (CSIM110, Sunny, Beijing, China).

2.11 Statistical analysis

All statistical analyses were conducted using GraphPad Prism 8 software (GraphPad Software Inc., San Diego, USA). To assess differences between data that followed a normal distribution, we conducted a

one-way analysis of variance (ANOVA) followed by Tukey's multiple comparison test. For data with non-normal distributions, the Kruskal–Wallis test was used, followed by a Dunn–Bonferroni test. To compare differences between two groups, an unpaired t-test was utilized, and for multiple comparisons, we used the Bonferroni correction for P values. A significance level of $P < 0.05$ was considered statistically significant.

3. Results

3.1 Activation of astrocytic Gq and Gi GPCRs mitigated impulsive-like behaviors and cognitive impairments in ADHD mice

To investigate the effects of astrocytic Gq and Gi GPCRs activation on ADHD mice, we initially ruled out any potential influence of CNO and the viral vector on the experiment (Figure S1 and S2). Notably, rAAV expression was confined to the astrocytes in the virally transduced region (Fig. 2A). The OFT results indicated that compared to the ADHD mice, both the ADHD + hM3Dq and ADHD + hM4Di groups exhibited a decrease in the total distance traveled, while the average speed did not show a significant difference among these three groups (Fig. 2B–D). In the EPM test, both the ADHD + hM3Dq and ADHD + hM4Di groups had a reduced percentage of time spent in the open arms compared to the ADHD mice (Fig. 2B–D). The NOR test results revealed that compared to the ADHD mice, both the ADHD + hM3Dq and ADHD + hM4Di groups had increased number of explorations of the novel object (Fig. 2G–H). In the FC experiment, compared to the ADHD mice, both the ADHD + hM3Dq and ADHD + hM4Di groups had increased context-related freezing time (Fig. 2I). Collectively, these findings suggest that the activation of astrocytic Gq and Gi GPCRs could improve impulsive behavior and cognitive impairments in ADHD mice.

3.2 Activation of astrocytic Gq and Gi GPCRs influenced neurophysiology

In typically developing infants, θ oscillation power activity has been associated with attention, cognitive control and working memory[22], and studies have indicated an increase in θ oscillation power in children with ADHD[23]. Therefore, we chose to focus our research on θ oscillation power. The NOR data indicated that compared to the ADHD mice, both the ADHD + hM3Dq and ADHD + hM4Di mice exhibited an increase in exploration time for the novel object. The neurophysiology results revealed a significant reduction in θ oscillation power in both the ADHD + hM3Dq and ADHD + hM4Di mice compared to the ADHD mice, with no significant difference observed between the ADHD + hM3Dq and ADHD + hM4Di mice (Fig. 2J–K). These findings suggest that the activation of astrocyte Gq and Gi GPCRs can inhibit the abnormal increase in θ oscillation power in ADHD mice.

3.3 Activation of astrocytic Gq and Gi GPCRs enhanced astrocyte activation, reduced the inflammatory response associated with pyroptosis

The research highlights the significance of the hippocampus, a crucial brain structure closely associated with functions such as learning, memory and emotional regulation[24]. Abnormalities in the hippocampus have been reported to be linked to executive function and cognitive control issues in individuals with ADHD[25−27]. The amygdala, another brain region intricately involved in emotion processing and emotional regulation, may also play a role in attention and emotional regulation problems in individuals with ADHD[28, 29]. Based on these considerations, we explored pathological changes in these regions. Histopathological findings indicated that compared to the ADHD mice, both the ADHD + hM3Dq and ADHD + hM4Di mice exhibited increased astrocyte activity, as indicated by GFAP intensity. Interestingly, GFAP intensity in the ADHD + hM3Dq mice was higher than that in the ADHD + hM4Di mice (Fig. 3A−D). Furthermore, both the ADHD + hM3Dq and ADHD + hM4Di mice showed an increase in GABAergic neuron activity, as indicated by GAD65 intensity, compared to the ADHD mice (Fig. 3A and E−G). Additionally, synaptic connectivity, represented by PSD95 intensity, was enhanced in both the ADHD + hM3Dq and ADHD + hM4Di mice compared to the ADHD mice (Fig. 3A and H−J). These results suggest that the activation of astrocytes, the reduction of inhibitory neurons and the enhancement of synaptic connectivity may alleviate impulsive behavior and cognitive impairments in ADHD mice. Furthermore, the data demonstrated that, compared with the ADHD mice, the expression of cleaved caspase-1 in astrocytes was down-regulated in the ADHD + hM3Dq and the ADHD + hM4Di mice (Fig. 5A-D). Additionally, there was a decrease in the expression levels of IL-18 compared to the ADHD mice (Fig. 5A and E-G). Earlier studies have shown that normal levels of IL-18 contribute to synaptic formation[30]. These data suggest that cognitive impairment may be associated with an inflammatory response in astrocytes associated with pyroptosis.

3.4 Astrocyte-specific NLRP3 knockout improved impulsive behavior and cognitive impairments in ADHD mice

Previous studies have indicated that NLRP3 is upregulated in ADHD models[17], and research has highlighted the significance of neuroinflammation as a significant risk factor for ADHD[16]. Consequently, astrocyte conditional knockout NLRP3 mice were generated for subsequent experiments through the breeding of NLRP3$^{f/f}$ mice with GFAP-Cre mice (Fig. 5A−C). Results from the OFT indicated that compared to the WT + ADHD mice, NLRP3-cKO + ADHD mice showed decreased total distance traveled, while the average speed did not show a significant difference between these two groups (Fig. 5D−F). In the EPM test, NLRP3-cKO + ADHD mice had reduced percentage of time spent in the open arms compared to the WT + ADHD mice (Fig. 5G−H). NOR data revealed that NLRP3-cKO + ADHD mice had increased number of explorations of the novel object compared to the WT + ADHD mice (Fig. 5I−J). In the FC experiment, NLRP3-cKO + ADHD mice demonstrated an increase in context-related freezing time in

contrast to the WT + ADHD mice (Fig. 2N). These data collectively suggest that astrocyte-specific NLRP3 knockout can ameliorate impulsive behavior and cognitive impairments in ADHD mice.

3.5 Astrocyte-specific NLRP3 knockout influenced neurophysiology

In the second stage of the NOR task, we utilized in vivo neurophysiological monitoring techniques to evaluate the activity of the hippocampal CA1 region in various groups of mice when exposed to a novel object. The results revealed a significant reduction in θ oscillation power in the NLRP3-cKO + ADHD mice when compared to the WT + ADHD mice (Fig. 5L-M). These findings suggest that astrocyte-specific NLRP3 knockout can effectively suppress the abnormal increase of θ oscillation power observed in ADHD mice.

3.6 Astrocyte-specific knockout enhanced astrocyte activation, reduced the inflammatory response associated with pyroptosis

Histopathological results revealed that compared to the WT + ADHD mice, NLRP3-cKO + ADHD mice exhibited an increase in GFAP intensity (Fig. 6A−D). Furthermore, NLRP3-cKO + ADHD mice showed enhanced GABAergic neuron activity, as indicated by increased GAD65 intensity compared to the WT + ADHD mice (Fig. 6A and E−G). Additionally, synaptic connectivity, represented by elevated PSD95 intensity, was observed in higher levels in NLRP3-cKO + ADHD mice compared to the WT + ADHD mice (Fig. 6A and H−J). These findings suggest that astrocyte-specific NLRP3 knockout, the reduction of inhibitory neurons and the enhancement of synaptic connectivity might contribute to the alleviation of impulsive behavior and cognitive impairments in ADHD mice. Moreover, the results indicated that the expression of cleaved caspase-1 in astrocytes was down-regulated in the NLRP3-cKO + ADHD mice compared to the WT + ADHD mice (Fig. 7A−D). Additionally, there was a decrease in the expression levels of IL-18 in the NLRP3-cKO + ADHD mice compared to the WT + ADHD mice (Fig. 6A and E−G). Previous studies have shown that normal levels of IL-18 contribute to synaptic formation[30]. Overall, these data suggest that cognitive impairment could be associated with an inflammatory response in astrocytes related to pyroptosis.

4. Discussion

Both the activation and inhibition of hippocampal CA1 astrocytes have demonstrated the potential to ameliorate impulsive-like behaviors in ADHD mice, alleviate cognitive impairments, reduce theta oscillation power during NOR and diminish NLRP3-associated inflammatory factors, including cleaved caspase-1 and IL-8. Additionally, compared to WT mice, astrocyte-specific NLRP3 conditional knockout mice showed significant reductions in impulsive behaviors and cognitive deficits, along with decreased theta oscillation power and attenuated NLRP3-associated inflammatory factors.

An increasing number of evidence highlights the pivotal role of astrocytic GPCRs in regulating cognitive and memory processes[31−33]. Prior research has demonstrated that selective stimulation of the Gi-GPCR pathway in striatal astrocytes can correct various astrocytic, synaptic and behavioral phenotypes related to Huntington's disease (HD) while improving signaling pathways associated with HD-related astrocytes, such as those linked to synaptic events and neuroimmune functions[34]. Additionally, studies have shown that the activation of astrocytic Gq-GPCR pathways can enhance synaptic transmission, facilitate memory allocation and improve memory performance[15]. These findings align with the results of our experiment, where the activation of Gq and Gi GPCRs enhances cognitive function in the model mice.

Our findings confirm that the activation of Gq and Gi GPCRs can mitigate NLRP3-induced pyroptosis, aligning with existing research indicating that alleviating neuroinflammation can ameliorate ADHD-like behaviors[17]. Notably, in our experiment, mice with activated Gq GPCRs displayed increased GFAP expression compared to mice with activated Gi GPCRs. This difference in GFAP expression could be attributed to variations in intracellular Ca^{2+} levels triggered by the activation of Gq and Gi GPCRs[35].

The experimental results revealed that mice with activated Gq and Gi GPCRs exhibited an increased expression of GAD65, which could have contributed to a reduction in GABA secretion, consequently leading to a diminished activation of $GABA_A$ receptors, ultimately resulting in a decrease in θ oscillation power. Notably, the $GABA_A$ receptor appears to play a pivotal role in the generation of induced θ oscillations[36]. Previous research has indicated that the augmentation of θ oscillation power can be hindered by the $GABA_A$ receptor antagonist[37]. Moreover, studies have demonstrated that the release of GABA, and subsequently the activation of $GABA_A$ receptors, can induce θ oscillations[38], consistent with the outcomes of our experiments. In the hippocampus, the GABAergic parvalbumin inhibition serves as the fundamental mechanism underlying the attenuation of θ oscillations, concurrently leading to an increased expression of PSD-95 in the hippocampus[39], similar to that observed in our present study.

Our research indicated that activation of Gq and Gi GPCRs can mitigate NLRP3-induced pyroptosis. Notably, Ca^{2+} mobilization is reported as an important upstream event in NLRP3 activation[40, 41]. Some scholars have demonstrated that the application of CNO to hippocampal slices transduced with Gi-DREADD effectively reduces intracellular baseline Ca^{2+} levels[42], in line with the results of our research. However, some studies indicated that activation of Gq GPCRs can increase Ca^{2+} levels[43], subsequently activating NLRP3, which contrasts with our research findings. However, the specific reasons for this discrepancy warrant further investigation. In this present study, we also conducted conditional NLRP3 knockout in astrocytes and observed its efficacy in alleviating ADHD symptoms in mice, which further elucidates the role of NLRP3-induced astrogliosis in ADHD, aligning with prior literature[17, 44].

This study had certain limitations. Firstly, the investigation was conducted for 21 days, and additional research is necessary to assess the potential age-related changes more comprehensively. Secondly, the use of the proprietary S-ketamine model in this study requires validation through alternative transgenic

models. Moreover, further research is needed to establish and validate the relationship between Gq-GPCR and calcium ions, particularly regarding their potential association with cellular apoptosis.

In summary, our current research highlights that the activation of Gq and Gi GPCRs can effectively alleviate hyperactivity and cognitive dysfunction in mice with ADHD-like symptoms, offering valuable insights for the development of potential clinical interventions for ADHD.

Declarations

Author contributions

YDS, WJG and LMZ were responsible for the design of the study. ZFY and GGL was responsible for statistical analysis. YDS, ZFY, GGL wrote the main manuscript text. YDS, YLS, BDL and JYZ were responsible for the experiments and data collection. YDS, WJG and LMZ confirmed the authenticity of all raw data. All authors have read and approved the final manuscript. All authors read and approved the final manuscript.

Funding

Availability of data and materials

The data generated and analyzed in this study are available from the corresponding author on reasonable request.

Ethics approval and consent to participate

The Hebei Province Cangzhou Hospital of Integrated Traditional and Western Medicine's Institutional Animal Care and Use Committee authorized all experimental techniques used in this study (No. CZX2023-KY-023).

Competing interests

The authors declare that they have no competing interests.

Author details

[1]Hebei Province Cangzhou Hospital of Integrated Traditional and Western Medicine, Cangzhou, China.

[2]Hebei Province Key Laboratory of Integrated Traditional and Western Medicine in Neurological Rehabilitation, Cangzhou, China.[3]The First Affiliated Hospital of Zhengzhou University, Henan,

China.[4]Hebei Key Laboratory of Integrated Traditional and Western Medicine in Osteoarthrosis Research (Preparing), Cangzhou, China.[5]Hebei Key Laboratory of Chinese Medicine Research on Cardio-Cerebrovascular Disease, Hebei University of Chinese Medicine, Shijiazhuang, China.

References

1. THAPAR A, COOPER M. Attention deficit hyperactivity disorder[J]. Lancet, 2016, 387(10024):1240–50.

2. SAYAL K, PRASAD V, DALEY D, et al. ADHD in children and young people: prevalence, care pathways, and service provision[J]. Lancet Psychiatry, 2018, 5(2):175–186.

3. BIEDERMAN J, MONUTEAUX M C, MICK E, et al. Young adult outcome of attention deficit hyperactivity disorder: a controlled 10-year follow-up study[J]. Psychol Med, 2006, 36(2):167–79.

4. CHANG Z, GHIRARDI L, QUINN P D, et al. Risks and Benefits of Attention-Deficit/Hyperactivity Disorder Medication on Behavioral and Neuropsychiatric Outcomes: A Qualitative Review of Pharmacoepidemiology Studies Using Linked Prescription Databases[J]. Biol Psychiatry, 2019, 86(5):335–343.

5. ZHANG L M, LIU N N, CAO L, et al. S-ketamine administration in pregnant mice induces ADHD- and depression-like behaviors in offspring mice[J]. Behav Brain Res, 2022, 433:113996.

6. SCHOBER A L, WICKI-STORDEUR L E, MURAI K K, et al. Foundations and implications of astrocyte heterogeneity during brain development and disease[J]. Trends Neurosci, 2022, 45(9):692–703.

7. ARMBRUSTER B N, LI X, PAUSCH M H, et al. Evolving the lock to fit the key to create a family of G protein-coupled receptors potently activated by an inert ligand[J]. Proc Natl Acad Sci U S A, 2007, 104(12):5163–8.

8. SUTHARD R L, JELLINGER A L, SURETS M, et al. Chronic Gq activation of ventral hippocampal neurons and astrocytes differentially affects memory and behavior[J]. Neurobiol Aging, 2023, 125:9–31.

9. AGULHON C, BOYT K M, XIE A X, et al. Modulation of the autonomic nervous system and behaviour by acute glial cell Gq protein-coupled receptor activation in vivo[J]. J Physiol, 2013, 591(22):5599–609.

10. JONES M E, PANICCIA J E, LEBONVILLE C L, et al. Chemogenetic Manipulation of Dorsal Hippocampal Astrocytes Protects Against the Development of Stress-enhanced Fear Learning[J]. Neuroscience, 2018, 388:45–56.

11. FRANKLAND P W, BONTEMPI B. The organization of recent and remote memories[J]. Nat Rev Neurosci, 2005, 6(2):119–30.

12. WHITLOCK J R, HEYNEN A J, SHULER M G, et al. Learning induces long-term potentiation in the hippocampus[J]. Science, 2006, 313(5790):1093–7.

13. MARTINUSSEN R, HAYDEN J, HOGG-JOHNSON S, et al. A meta-analysis of working memory impairments in children with attention-deficit/hyperactivity disorder[J]. J Am Acad Child Adolesc

Psychiatry, 2005, 44(4):377−84.

14. PIñA R, ROZAS C, CONTRERAS D, et al. Atomoxetine Reestablishes Long Term Potentiation in a Mouse Model of Attention Deficit/Hyperactivity Disorder[J]. Neuroscience, 2020, 439:268−274.

15. ADAMSKY A, KOL A, KREISEL T, et al. Astrocytic Activation Generates De Novo Neuronal Potentiation and Memory Enhancement[J]. Cell, 2018, 174(1):59−71.e14.

16. HAN V X, PATEL S, JONES H F, et al. Maternal immune activation and neuroinflammation in human neurodevelopmental disorders[J]. Nat Rev Neurol, 2021, 17(9):564−579.

17. ABU-ELFOTUH K, ABDEL-SATTAR S A, ABBAS A N, et al. The protective effect of thymoquinone or/and thymol against monosodium glutamate-induced attention-deficit/hyperactivity disorder (ADHD)-like behavior in rats: Modulation of Nrf2/HO-1, TLR4/NF-κB/NLRP3/caspase-1 and Wnt/β-Catenin signaling pathways in rat model[J]. Biomed Pharmacother, 2022, 155:113799.

18. SALEM H A, ELSHERBINY N, ALZAHRANI S, et al. Neuroprotective Effect of Morin Hydrate against Attention-Deficit/Hyperactivity Disorder (ADHD) Induced by MSG and/or Protein Malnutrition in Rat Pups: Effect on Oxidative/Monoamines/Inflammatory Balance and Apoptosis[J]. Pharmaceuticals (Basel), 2022, 15(8).

19. ZHANG L M, ZHANG D X, SONG R X, et al. IL-18BP Alleviates Anxiety-Like Behavior Induced by Traumatic Stress via Inhibition of the IL-18R-NLRP3 Signaling Pathway in a Mouse Model of Hemorrhagic Shock and Resuscitation[J]. Mol Neurobiol, 2023, 60(1):382−394.

20. KIM J H, RAHMAN M H, LEE W H, et al. Chemogenetic stimulation of the G(i) pathway in astrocytes suppresses neuroinflammation[J]. Pharmacol Res Perspect, 2021, 9(6):e00822.

21. XIE A X, MADAYAG A, MINTON S K, et al. Sensory satellite glial Gq-GPCR activation alleviates inflammatory pain via peripheral adenosine 1 receptor activation[J]. Sci Rep, 2020, 10(1):14181.

22. OREKHOVA E V, STROGANOVA T A, POSIKERA I N, et al. EEG theta rhythm in infants and preschool children[J]. Clin Neurophysiol, 2006, 117(5):1047−62.

23. YORDANOVA J, HEINRICH H, KOLEV V, et al. Increased event-related theta activity as a psychophysiological marker of comorbidity in children with tics and attention-deficit/hyperactivity disorders[J]. Neuroimage, 2006, 32(2):940−55.

24. SAHAY A, SCOBIE K N, HILL A S, et al. Increasing adult hippocampal neurogenesis is sufficient to improve pattern separation[J]. Nature, 2011, 472(7344):466−70.

25. POLLI F S, IPSEN T H, CABALLERO-PUNTIVERIO M, et al. Cellular and Molecular Changes in Hippocampal Glutamate Signaling and Alterations in Learning, Attention, and Impulsivity Following Prenatal Nicotine Exposure[J]. Mol Neurobiol, 2020, 57(4):2002−2020.

26. UGARTE G, PIñA R, CONTRERAS D, et al. Attention Deficit-Hyperactivity Disorder (ADHD): From Abnormal Behavior to Impairment in Synaptic Plasticity[J]. Biology (Basel), 2023, 12(9).

27. MURTHY S, KANE G A, KATCHUR N J, et al. Perineuronal Nets, Inhibitory Interneurons, and Anxiety-Related Ventral Hippocampal Neuronal Oscillations Are Altered by Early Life Adversity[J]. Biol Psychiatry, 2019, 85(12):1011−1020.

28. SEGUIN D, PAC S, WANG J, et al. Amygdala subnuclei volumes and anxiety behaviors in children and adolescents with autism spectrum disorder, attention deficit hyperactivity disorder, and obsessive-compulsive disorder[J]. Hum Brain Mapp, 2022, 43(16):4805–4816.

29. SONG S, QIU J, LU W. Predicting disease severity in children with combined attention deficit hyperactivity disorder using quantitative features from structural MRI of amygdaloid and hippocampal subfields[J]. J Neural Eng, 2021, 18(4).

30. TZENG T C, HASEGAWA Y, IGUCHI R, et al. Inflammasome-derived cytokine IL18 suppresses amyloid-induced seizures in Alzheimer-prone mice[J]. Proc Natl Acad Sci U S A, 2018, 115(36):9002–9007.

31. SANTELLO M, TONI N, VOLTERRA A. Astrocyte function from information processing to cognition and cognitive impairment[J]. Nat Neurosci, 2019, 22(2):154–166.

32. KOL A, GOSHEN I. The memory orchestra: the role of astrocytes and oligodendrocytes in parallel to neurons[J]. Curr Opin Neurobiol, 2021, 67:131–137.

33. HENNEBERGER C, BARD L, PANATIER A, et al. LTP Induction Boosts Glutamate Spillover by Driving Withdrawal of Perisynaptic Astroglia[J]. Neuron, 2020, 108(5):919–936.e11.

34. YU X, NAGAI J, MARTI-SOLANO M, et al. Context-Specific Striatal Astrocyte Molecular Responses Are Phenotypically Exploitable[J]. Neuron, 2020, 108(6):1146–1162.e10.

35. VAN DEN HERREWEGEN Y, SANDERSON T M, SAHU S, et al. Side-by-side comparison of the effects of Gq- and Gi-DREADD-mediated astrocyte modulation on intracellular calcium dynamics and synaptic plasticity in the hippocampal CA1[J]. Mol Brain, 2021, 14(1):144.

36. LU C B, LI C Z, LI D L, et al. Nicotine induction of theta frequency oscillations in rodent medial septal diagonal band in vitro[J]. Acta Pharmacol Sin, 2013, 34(6):819–29.

37. XING H, XU S, XIE X, et al. Levetiracetam induction of theta frequency oscillations in rodent hippocampus in vitro[J]. Can J Physiol Pharmacol, 2020, 98(10):725–732.

38. AVOLI M. Inhibition, oscillations and focal seizures: An overview inspired by some historical notes[J]. Neurobiol Dis, 2019, 130:104478.

39. RADOVANOVIC L, NOVAKOVIC A, PETROVIC J, et al. Different Alterations of Hippocampal and Reticulo-Thalamic GABAergic Parvalbumin-Expressing Interneurons Underlie Different States of Unconsciousness[J]. Int J Mol Sci, 2023, 24(7).

40. MURAKAMI T, OCKINGER J, YU J, et al. Critical role for calcium mobilization in activation of the NLRP3 inflammasome[J]. Proc Natl Acad Sci U S A, 2012, 109(28):11282–7.

41. LEE G S, SUBRAMANIAN N, KIM A I, et al. The calcium-sensing receptor regulates the NLRP3 inflammasome through Ca2 + and cAMP[J]. Nature, 2012, 492(7427):123–7.

42. KOL A, ADAMSKY A, GROYSMAN M, et al. Astrocytes contribute to remote memory formation by modulating hippocampal-cortical communication during learning[J]. Nat Neurosci, 2020, 23(10):1229–1239.

43. MARTIN-FERNANDEZ M, JAMISON S, ROBIN L M, et al. Synapse-specific astrocyte gating of amygdala-related behavior[J]. Nat Neurosci, 2017, 20(11):1540–1548.

44. ABU-ELFOTUH K, DARWISH A, ELSANHORY H M A, et al. In silico and in vivo analysis of the relationship between ADHD and social isolation in pups rat model: Implication of redox mechanisms, and the neuroprotective impact of Punicalagin[J]. Life Sci, 2023, 335:122252.
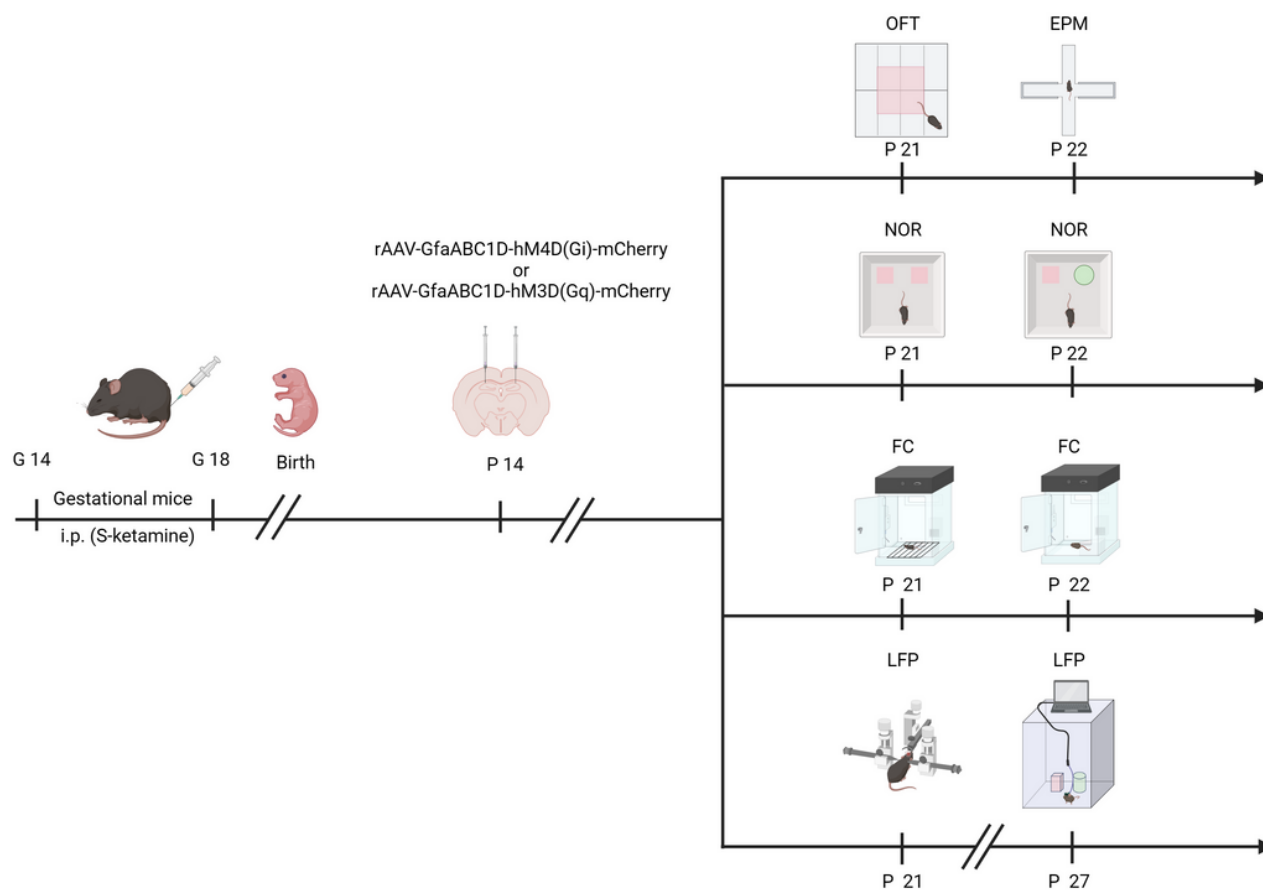
Figures

Figure 1

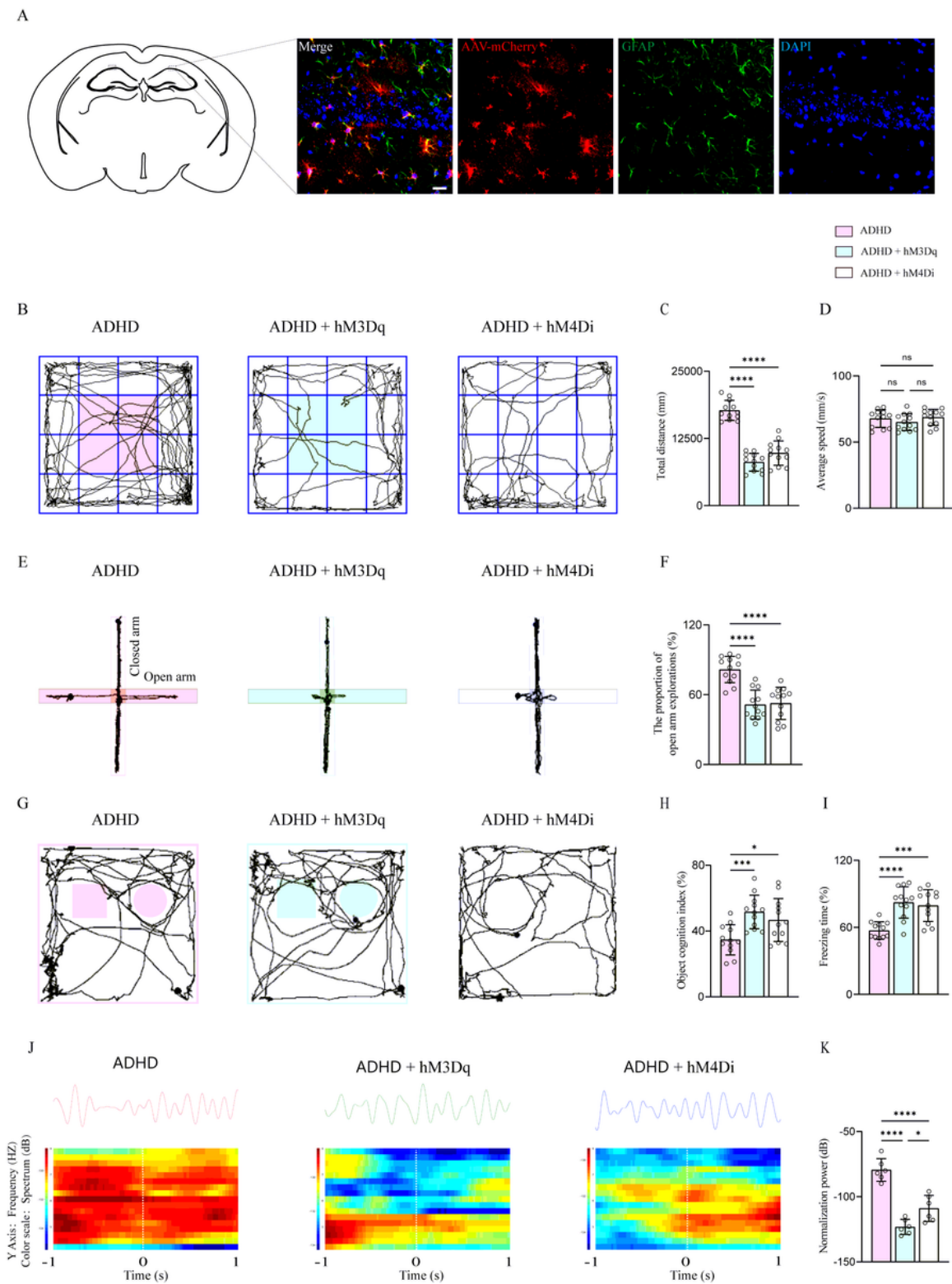**Experimental schematic diagram** (created using BioRender.com).

Figure 2

Activation of astrocytic Gq and Gi GPCRs improves impulsive behavior and cognitive impairments in ADHD mice. (A) Selective astrocytic expression of rAAV in the virally transduced CA1 region. Scale bar = 40 μm. (B) Trajectories from OFT showing movement patterns induced by indicated stimuli at 21 days post-birth. (C-D) Total distance traveled and average speed during the OFT. Data are mean ± SD (n = 12 mice per group). (E) Trajectories from the EPM illustrating movement responses to indicated stimuli at 22

days post-birth. (F) Percentage of open-arm explorations in the EPM. Data are shown as mean ± SD (n = 12 mice per group). (G) Trajectories from the NOR task, showing movement responses to indicated stimuli at 21-22 days post-birth. (H) Object cognition index in NOR. Data are shown as mean ± SD (n = 12 mice per group). (I) Freezing time during fear conditioning. Data are shown as mean ± SD (n = 12 mice). (J) Power spectrum of mouse LFP data in the theta band. (K) Mean theta power during exploration of the novel location. Data are shown as mean ± SD (n = 6 mice per group).
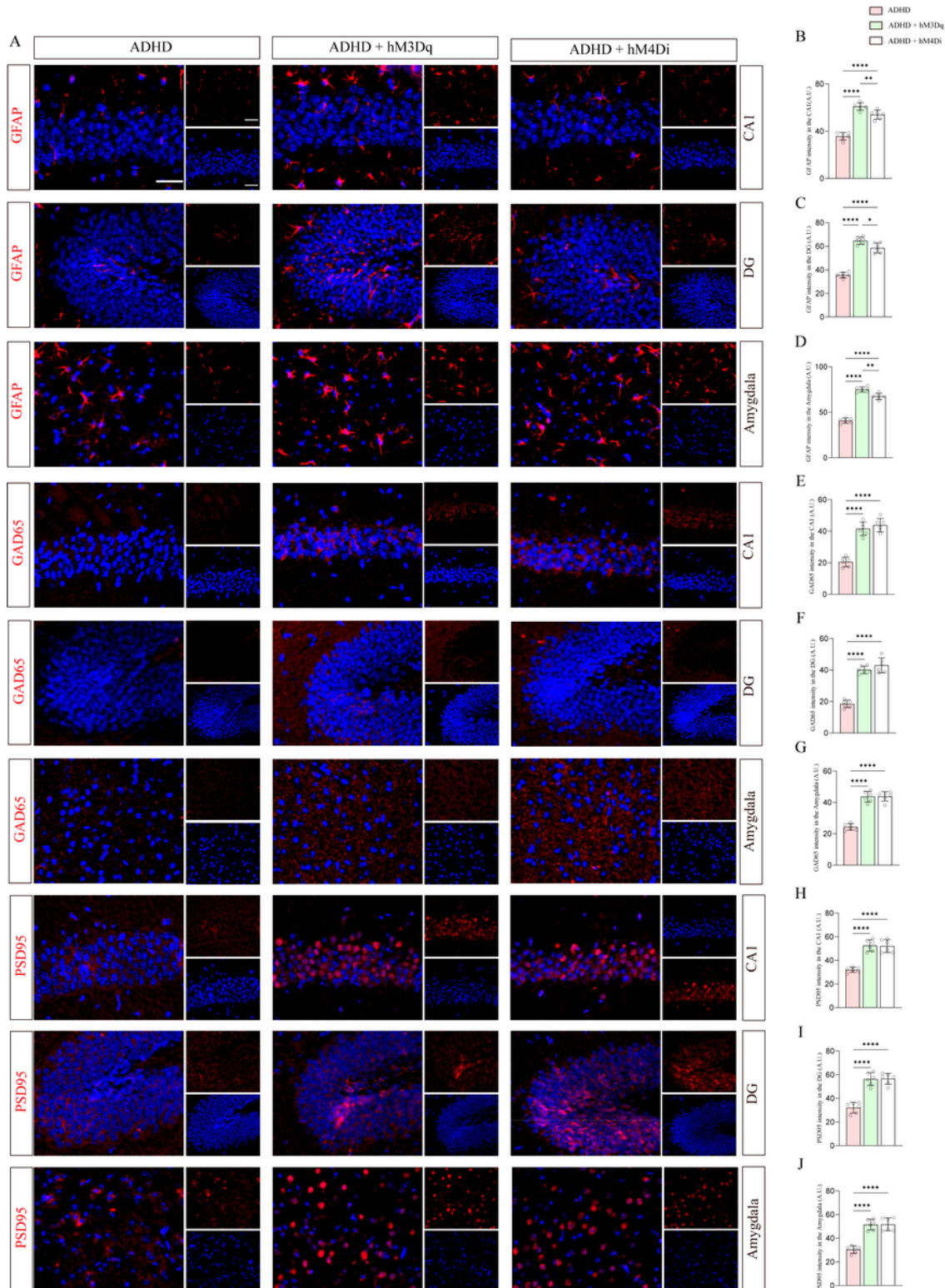
Figure 3

Activation of astrocytic Gq and Gi GPCRs enhances astrocyte activation, increases GABAergic neuron activity, and augments synaptic connectivity. (A) Representative photomicrographs in the CA1, DG, amygdala, at 23 days post-birth. Scale bar = 40 μm. (B-J) Quantification of GFAP, GAD65, and PSD95 intensity in each group. Data are presented as the mean ± SD (n = 6 mice per group).
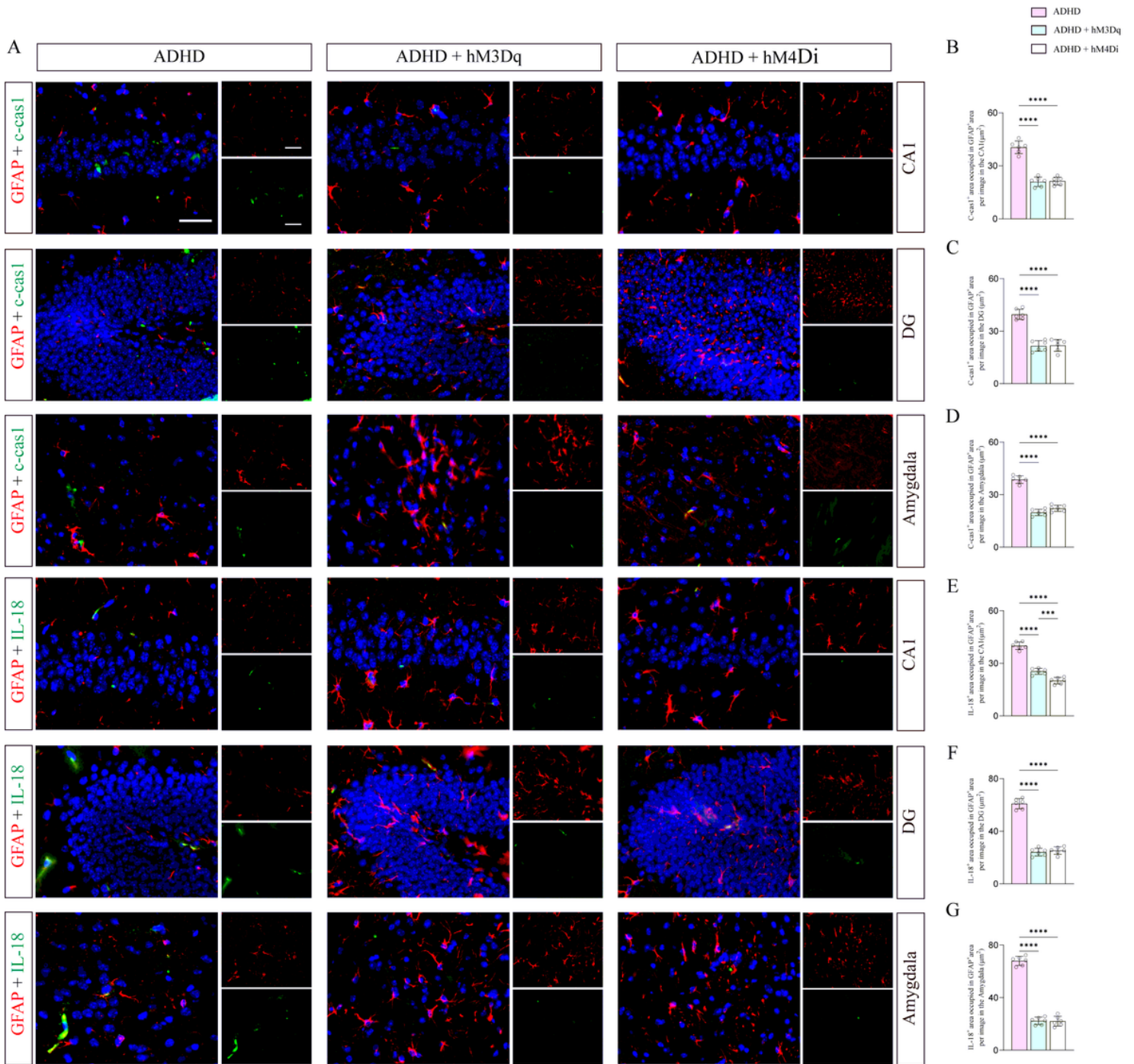

Figure 4

Astrocytic Gq and Gi GPCR activation reduces the inflammatory response associated with pyroptosis in astrocytes. (A) Representative photomicrographs in the CA1, DG, amygdala, at 23 days post-birth. Scale

bar = 40 μm. (B-D) Co-stained area of cleaved caspase-1- and GFAP-positive cells. Data are presented as the mean ± SD (n = 6 mice per group). (E-G) Co-stained area of IL-18- and GFAP-positive cells. Data are presented as the mean ± SD (n = 6 mice per group).
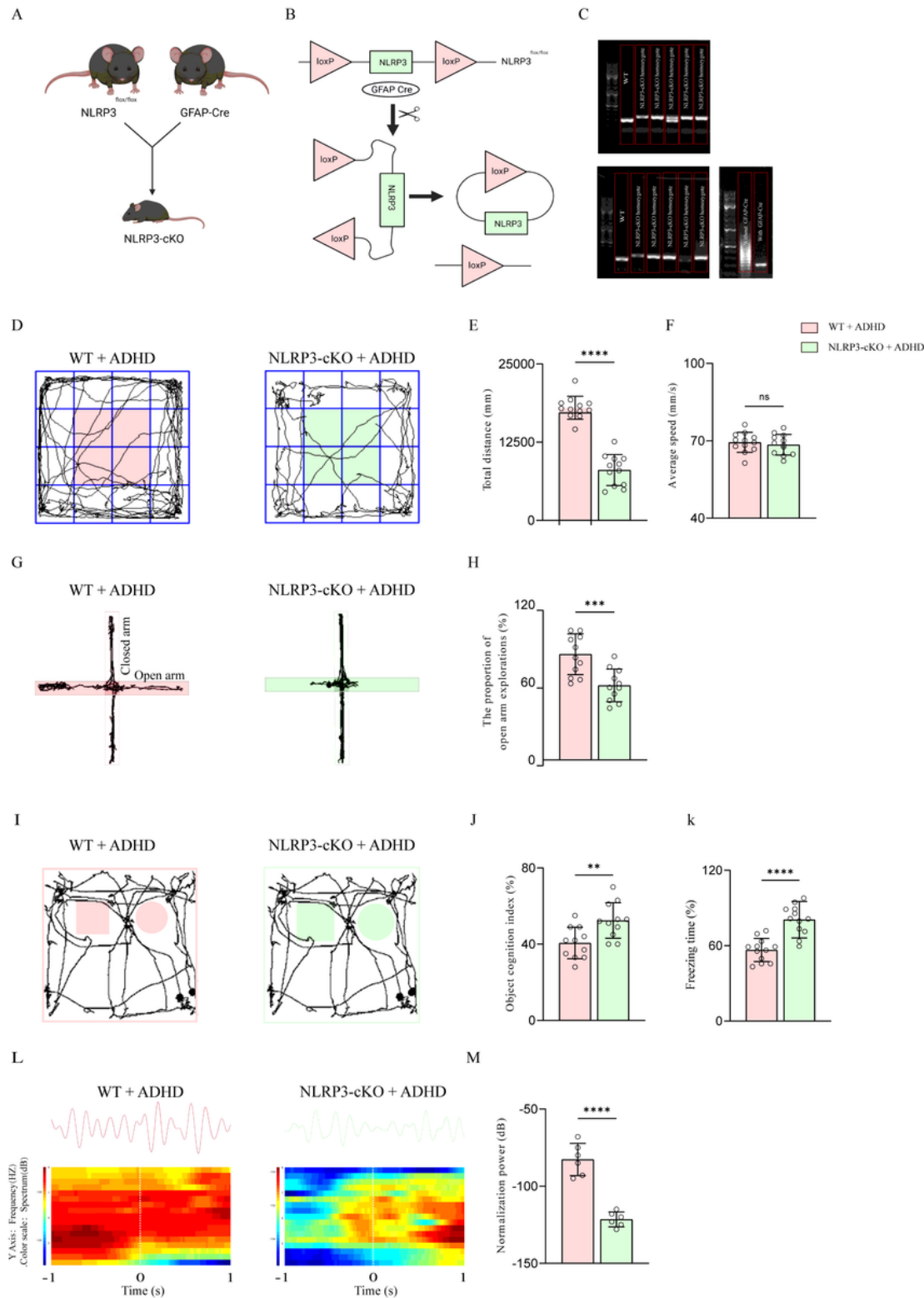

Figure 5

Astrocyte-specific NLRP3 knockout improves impulsive behavior and cognitive impairments in ADHD mice. (A-B) Breeding scheme of GFAP-Cre mice crossed with NLRP3-cKO mice and the genetic strategy for generating NLRP3-cKO mice (createdwith BioRender.com). (C) Representative genotyping analysis for NLRP3-cKO homozygote, NLRP3-cKO heterozygote, and WT (wild type) mice and NLRP3-cKO homozygote, NLRP3-cKO heterozygote, GFAP-Cre, non-GFAP-Cre mice.(D) Computer printouts of shift trajectories generated from the OFT movement caused by the indicated stimuli at 21 days post-birth. (E-F) The total distance and average speed in the OFT. Data are presented as the mean ± SD (n = 12 mice per group). (G) Computer printouts of shift trajectories generated from the EPM movement caused by the indicated stimuli at 22 days post-birth. (H) The proportion of open arm explorations in the EPM. Data are presented as the mean ± SD (n = 12 mice per group). (I) Computer printouts of shift trajectories generated from the NOR movement caused by the indicated stimuli at 21-22 days post-birth. (J) Object cognition index in NOR. Data are presented as the mean ± SD (n = 12 mice per group). (k) Freezing time in fear conditioning. Data are presented as the mean ± SD (n = 12) (L) Power spectrum of the mice LFP data at the theta band. (M) Mean theta power while the mice explored the novel location. Data are presented as the mean ± SD (n = 6 mice per group).
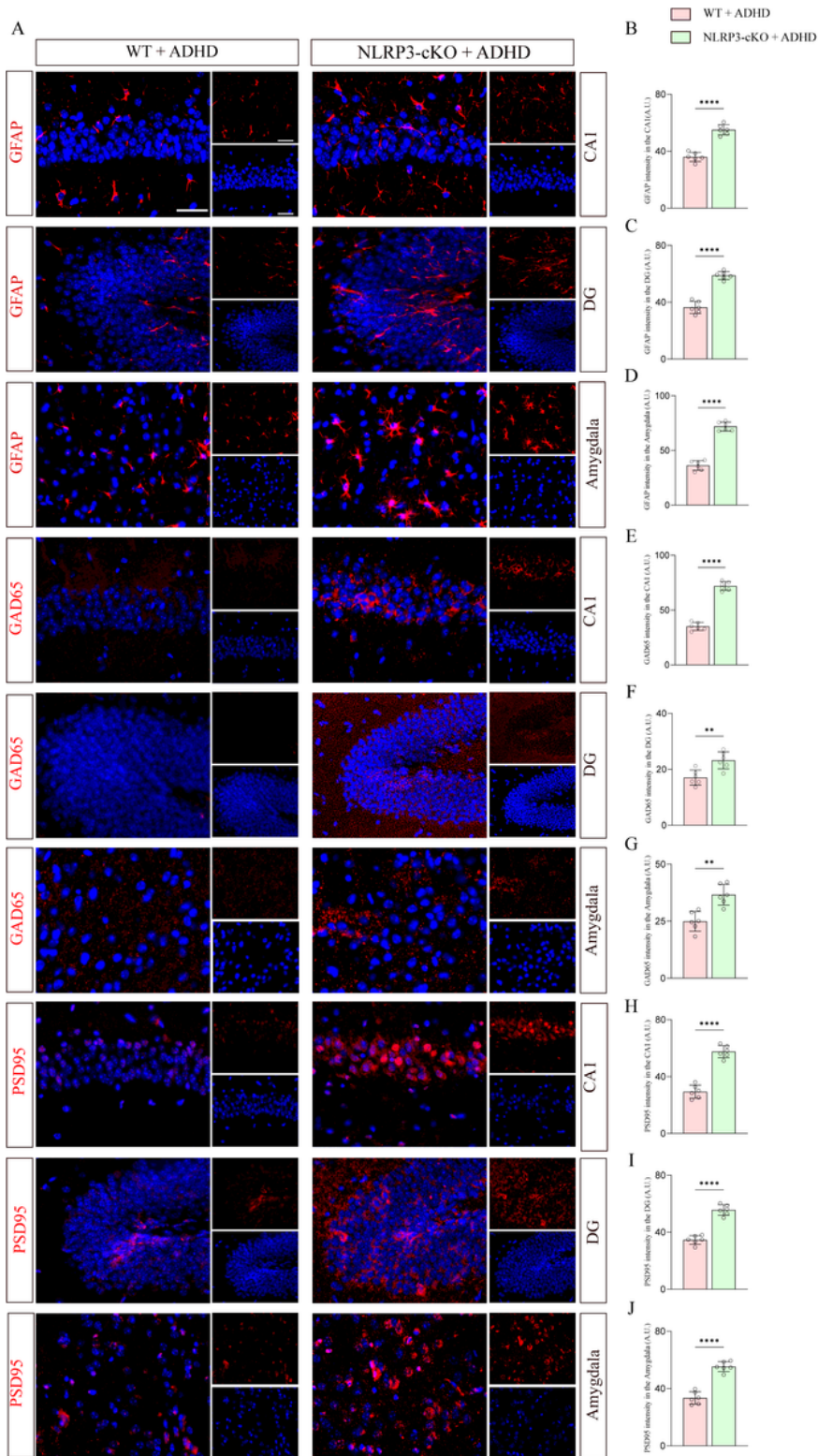
Figure 6

Astrocyte-specific NLRP3 knockout enhances astrocyte activation, increases GABAergic neuron activity, and augments synaptic connectivity. (A) Representative photomicrographs in the CA1, DG, amygdala, at 23 days post-birth. Scale bar = 40 μm. (B-J) The intensity of GFAP, GAD65, and PSD95 was quantified in each group. Data are presented as the mean ± SD (n = 6 mice per group).
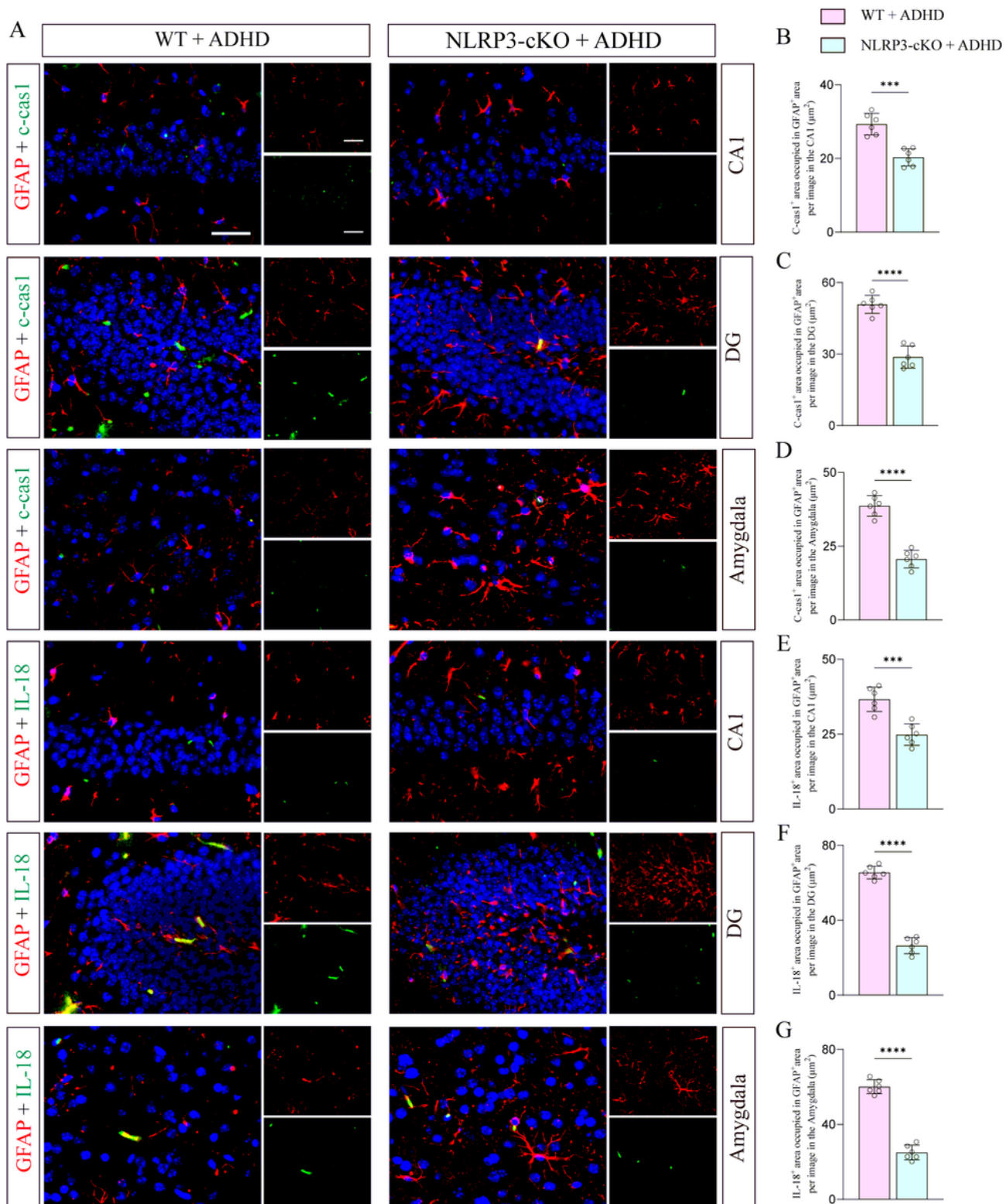
Figure 7

Astrocyte-specific NLRP3 knockout reduces the inflammatory response associated with pyroptosis in astrocytes. (A) Representative photomicrographs in the CA1, DG, amygdala, at 23 days post-birth. Scale bar = 40 μm. (B-D) Co-stained area of cleaved caspase-1- and GFAP-positive cells. Data are presented as the mean ± SD (n = 6 mice per group). (E-G) Co-stained area of IL-18- and GFAP-positive cells. Data are presented as the mean ± SD (n = 6 mice per group).

Supplementary Files

This is a list of supplementary files associated with this preprint. Click to download.

- Supplementalfile1.docx
- Supplementalfile2.docx